Potential Role of Zinc Dyshomeostasis in Matrix Metalloproteinase-2 and -9 Activation and Photoreceptor Cell Death in Experimental Retinal Detachment

Jeong A Choi,[1] Yoon Jeon Kim,[2] Bo-Ra Seo,[1] Jae-Young Koh,[1,3] and Young Hee Yoon[2]

[1]Neural Injury Research Center, Asan Institute for Life Sciences, University of Ulsan College of Medicine, Seoul, Korea
[2]Department of Ophthalmology, University of Ulsan College of Medicine, Seoul, Korea
[3]Department of Neurology, Asan Medical Center, University of Ulsan College of Medicine, Seoul, Korea

Correspondence: Young Hee Yoon, Department of Ophthalmology, Asan Medical Center, University of Ulsan College of Medicine, 88, Olympic-ro 43-gil, Songpa-gu, Seoul, Korea 05505;
yhyoon@amc.seoul.kr.

JC and YJK contributed equally to the work presented here and should therefore be regarded as equivalent authors.

Submitted: November 28, 2017
Accepted: May 22, 2018

Citation: Choi J, Kim YJ, Seo B-R, Koh J-Y, Yoon YH. Potential role of zinc dyshomeostasis in matrix metalloproteinase-2 and -9 activation and photoreceptor cell death in experimental retinal detachment. *Invest Ophthalmol Vis Sci*. 2018;59:3058–3068. https://doi.org/10.1167/iovs.17-23502

Purpose. We investigated whether zinc dyshomeostasis, a known mechanism of cell death in acute brain injury, contributes to the activation of matrix metalloproteinases (MMPs) and photoreceptor cell death in experimental retinal detachment (RD).

Methods. RD was induced in mice by subretinal injection of 1:1 mixture of balanced salt solution and 1% sodium hyaluronate. On days 1 and 3 post RD, eyeballs were sectioned and examined for cell death (TUNEL staining), the degree of hypoxic insult (Hypoxyprobe staining), free zinc levels (TFL-Zn staining), and MMP-2 and -9 activity (gelatin zymography). In addition, we examined whether modulating extracellular zinc concentration or MMP activation in subretinal fluid affected photoreceptor cell death in RD. These changes were further examined in primary retinal cell and photoreceptor-derived cell (661W) cultures.

Results. Photoreceptor cell death peaked on day 3 post RD. Intracellular zinc markedly decreased on day 1 post RD, and subsequently accumulated on day 3. MMP-2 and -9 activity showed a concurrent increase in detached retinas. Detached retinas stained with Hypoxyprobe showed strongly positive cells, especially in the photoreceptor layer. Subretinal injection of a zinc-chelator (CaEDTA) or MMP inhibitor (GM6001, minocycline) at the time of RD significantly attenuated photoreceptor cell death in RD. Similar findings were confirmed in oxygen-glucose–deprived or zinc-exposed cell cultures.

Conclusions. Upon RD, hypoxic retinal cells in deep layers underwent zinc dyshomeostasis, MMP activation, and ultimately death. These findings provide new insight into the possible mechanism of photoreceptor death in RD, and as such may prove useful in crafting protective measures for photoreceptor cells.

Keywords: matrix metalloproteinase (MMP), photoreceptor cell death, retinal detachment, zinc dyshomeostasis

Despite significant advances in surgical management, the visual acuity of patients with rhegmatogenous retinal detachment (RD) is not always restored, even after a successful operation.[1] It has been postulated that photoreceptor cell apoptosis is the main reason for such vision loss.[2,3] Thus, a number of studies have sought to elucidate the pathomechanism of photoreceptor cell degeneration and thereby identify possible neuroprotective measures against photoreceptor cell death.[4–8]

RD triggers extensive morphologic changes in retinal tissue, which is followed by tissue remodeling. Matrix metalloproteinases (MMPs)—zinc-dependent enzymes that degrade extracellular matrix proteins—play a critical role in tissue remodeling, and studies have demonstrated elevated MMP-2 and MMP-9 activity in subretinal fluid (SRF, the accumulated fluid beneath the retina in cases of RD) obtained from patients with RD.[9,10] Although the sources and activation mechanism of MMPs in SRF are yet to be determined, MMPs are generally secreted as inactive proenzymes that are activated by zinc via a cysteine-switch mechanism.[11] Because MMP activation can cause cell death in a variety of contexts, it has been proposed that such increases in MMP activity in RD contribute to RD-induced photoreceptor cell death.

Zinc, the most abundant trace element in the eye, plays important roles in a wide range of physiological and pathologic processes.[12] Dysregulation of zinc homeostasis has been implicated in the pathophysiology of many acute neural injuries and chronic neurodegenerative diseases. Because changes in free zinc levels may modulate the activity of MMPs,[13] it is conceivable that zinc might participate in the increase in MMP activity, and thereby contribute to the photoreceptor cell death that occurs in RD. In addition, zinc dyshomeostasis in photoreceptor cells per se may trigger cell death cascades.[14] Despite the potential importance of zinc-dependent injury cascades in the pathophysiology of RD, few studies have been conducted to address this possibility. Hence, in the present study, we sought to investigate the involvement of zinc dyshomeostasis in photoreceptor cell death in an experimental model of RD in mice.

Methods

Experimental Animals

All animal experiments adhered to the ARVO Statement for the Use of Animals in Ophthalmic and Vision Research, and the protocols were approved by the Internal Review Board for Animal Experiments of the Asan Life Science Institute, University of Ulsan College of Medicine (Seoul, Korea). Male, 8-week-old, C57BL/6N mice weighing 22 to 25 g were purchased from Orient Bio, Inc. (Seoul, Korea). Animals were fed standard laboratory chow and were allowed free access to water in an air-conditioned room maintained at 24°C ± 0.5°C under a 12-hour light/dark cycle.

Chemicals

Calcium disodium EDTA (CaEDTA) and Minocycline were purchased from Sigma-Aldrich Corp. (St. Louis, MO, USA). GM6001 was purchased from TOCRIS Bioscience (Bristol, UK).

Retinal Detachment Induction

RD was created in the right eye of each animal as previously described[15,16]; the left eye served as control. Mice were anesthetized by inhalation of 1.5% isoflurane in a 1:3 mixture of O_2 and N_2O, administered at a flow rate of 2.0 l/min via a facemask connected to a coaxial circuit. Pupils were dilated with topical phenylephrine (5%) and tropicamide (0.5%) (Mydrin-P; Santen, Osaka, Japan); one drop of 0.5% proparacaine hydrochloride ophthalmic solution (Alcaine; Alcon Laboratories, Fort Worth, TX, USA) was applied to the eye as a topical anesthetic. The temporal conjunctiva at the posterior limbus was incised and detached from the sclera. A 30-gauge needle with the bevel pointed up was used to create a sclerotomy 1 mm posterior to the limbus. A scleral tunnel was created, followed by scleral penetration into the choroid, which makes a self-sealing scleral wound. A corneal puncture was made with a 30-gauge needle to lower intraocular pressure. A 33-gauge needle connected to a 10-μL Hamilton syringe was inserted into the subretinal space with the bevel pointed down. Then, 3 μL of 1:1 mixture of balanced salt solution (BSS) and 1% sodium hyaluronate (Healon; Advanced Medical Optics, Santa Ana, CA, USA) was injected gently, detaching the neurosensory retina from the underlying retinal pigment epithelium (RPE). We used a mixture of BSS and Healon instead of BSS only to prevent the retina from being reattached too quickly. Also, using a mixture of BSS and Healon instead of Healon only allowed us to precisely control the drug concentration in the subretinal space. To make the desired concentration of drug, we made 2-fold concentration of drugs dissolved in BSS, and mixed them with the same amount of Healon. Extracellular zinc concentrations in the subretinal space were modulated by using CaEDTA diluted in 1:1 mixture of BSS and Healon during generation of the RD model. To reduce MMP activation in RD, we administered GM6001 or minocycline (1 mM), mixed in the fluid injected into the subretinal space at the time of RD formation, followed by daily intraperitoneal injection. Formation of a reproducible bullous RD was confirmed by photographing the fundus using the Micron III retinal imaging system (Phoenix Research Laboratories, Inc., Pleasanton, CA, USA). Any animals that experienced surgical complications were excluded from the study.

Hematoxylin and Eosin Staining

Whole eye sections (10-μm thick) were prepared by using a cryostat and mounted onto glass slides coated with poly-L-lysine. After fixation with 4% paraformaldehyde (PFA), eye sections were stained with hematoxylin and eosin (H&E), mounted on glass slides, and examined for morphologic differences.

TUNEL Assay

In preparation for staining, eyes were enucleated, embedded in OCT compound (Tissue-Tek; Sakura Finetec, Torrance, CA, USA), cut into 10-μm-thick sections on a cryostat at −20°C, and mounted on prechilled glass slides coated with poly-L-lysine. The degree of apoptosis in eye sections was determined by performing terminal deoxynucleotidyl transferase–mediated fluorescein-16-dUTP nick-end labeling (TUNEL) assays, as described by the manufacturer (Roche, Basel, Switzerland). Briefly, frozen sections were fixed with 4% PFA for 30 minutes at room temperature. After permeabilization with 0.1% Triton X-100 in distilled water containing 0.1% sodium citrate, sections were stained by incubating in a nucleotide mixture containing fluorescein-12-dUTP and TdT (terminal transferase) at 37°C for 60 minutes. Nuclei were counterstained with DAPI (4′,6-diamidino-2-phenylindole).

MMP Zymography

Protein in retinal tissue or primary retinal cell lysates was quantified, and equal amounts of protein were incubated with Gelatin-Sepharose 4B (GE Healthcare, Uppsala, Sweden) for purification. Each pellet was washed with RIPA buffer and then electrophoresed on 10% Zymogram (Gelatin) gels (Novex-Invitrogen, Carlsbad, CA, USA). The active forms of MMP-9 and MMP-2 were visualized on gels by using Coomassie Blue staining. MMP activity was quantified densitometrically with ImageJ software (http://imagej.nih.gov/ij/; provided in the public domain by the National Institutes of Health, Bethesda, MD, USA).

Staining of Hypoxic Cells in Retinal Flat Mounts

One or 3 days after RD induction, mice were anesthetized by isoflurane (1.5%) inhalation, and hypoxic cells were stained by using a Hypoxyprobe-1 Plus Kit (Hypoxyprobe, Inc., Burlington, MA, USA). RD mice were injected retro-orbitally with Hypoxyprobe-1 (pimonidazole HCl, 60 mg/kg body weight). Forty-five minutes after Hypoxyprobe-1 administration, eyes were harvested and fixed by incubating in 4% PFA for 30 minutes at room temperature. After fixing, retinas were washed in phosphate-buffered saline (PBS), permeabilized by incubating in a solution consisting of PBS containing 0.2% Triton X-100, and then blocked with 5% goat serum in PBS. After incubation with fluorescein isothiocyanate (FITC)–conjugated MAb1 primary antibody (1:500) at 4°C for 24 hours, tissues were further incubated with horseradish peroxidase–conjugated rabbit anti-FITC secondary antibody (1:250). Tissues were examined by confocal microscopy (Carl-Zeiss, Oberkochen, Germany) and photographed.

TFL-Zinc Staining

Free or labile zinc in retinal tissues was detected by staining unfixed eyeball sections with the zinc-specific fluorescent dye N-(6-methoxy-8-quinolyl)-p-carboxybenzoyl-sulphonamide (TFL-Zn; Calbiochem, La Jolla, CA, USA), dissolved in Tris buffer (0.1 mM, pH 8.0).[17] After washing with PBS, TFL-Zn–stained sections were examined under a fluorescence microscope.

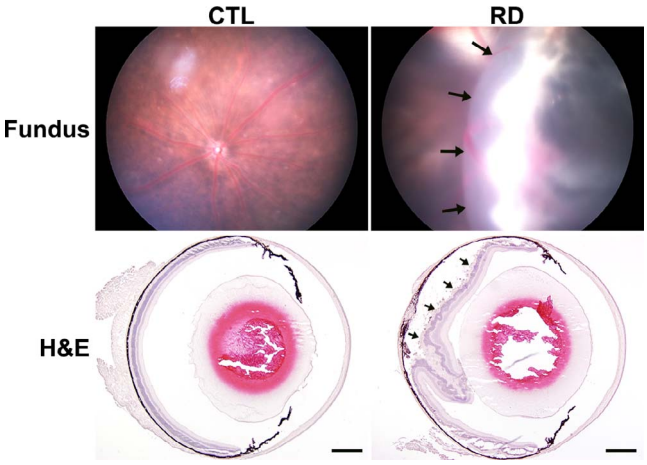

FIGURE 1. Establishment of experimental RD in mice. Representative images of experimentally induced RD in mice. *Upper*: Micron III fundus photographs showing elevated retinal tissue; *arrows* indicate the margin of detachment (*right*). *Lower*: Eyeball section stained with H&E, demonstrating that the retina was separated from the RPE (*arrows*, *right*). Original magnification, ×40; *scale bar*: 500 μm.

Measurement of Zinc Concentration in Retinal Tissues

Retinas of eyes from the RD experimental group and control eyes without RD were dissected from the eyeball. Zinc level in total retinal lysates was evaluated by using a Zinc Assay Kit (Metallo assay kit for Zinc LS; Metallogenics, Iwate, Japan) according to the provided protocol.

Primary Retinal Cell Culture

Primary retinal cell cultures, which included neurons, astrocytes, and photoreceptor cells, were prepared from the retinas of postnatal day 3 Sprague-Dawley rats, as described previously.[14,18] Briefly, retinas were isolated, placed in Ca^{2+}- and Mg^{2+}-free Hanks' balanced salt solution, and mechanically dissociated into single-cell suspensions by triturating with a pipette. Dissociated cells were suspended in Eagle's minimum essential medium (Invitrogen-Gibco, Grand Island, NY, USA) supplemented with 10% fetal bovine serum (FBS; HyClone Laboratories, Logan, UT, USA), 10% horse serum (Invitrogen), 2 mM L-glutamine, and penicillin-streptomycin (100 IU/mL-100 μg/mL; Lonza, Allendale, NJ, USA) and plated on poly- L-lysine–coated 24- or 6-well plates. Retinal cultures were maintained at 37°C in a humidified 5% CO_2 incubator, and used in experiments after culturing for 7 to 10 days in vitro.

Photoreceptor-Derived Cell Culture

The photoreceptor-derived cell line 661W, kindly provided by Muayyad R. Al-Ubaidi (University of Oklahoma, Oklahoma City, OK, USA), was maintained in Dulbecco's modified Eagle's medium (Invitrogen) containing 10% FBS and 1% penicillin-streptomycin. Cells were maintained at 37°C in a humidified 5% CO_2 incubator and were used after reaching approximately 80% confluence.

Oxygen-Glucose Deprivation

Oxygen-glucose deprivation (OGD) conditions were generated by incubating 661W cell line with OGD solution (Earle's balanced salt solution) for 3 or 6 hours at 37°C in a humidified 1% O_2 hypoxia incubator. OGD solution was generated by 116 mM NaCl, 5.4 mM KCl, 8 mM MgSO4, 10 mM NaH2PO4, 26.2 mM NaHCO3, and 10 μM glycine in distilled water. Before use, the OGD solution was bubbled (used mixed gas, composition: CO_2 5%, N_2 95%) and Dissolved Oxygen kit (CHEMets kit) was used to confirm its oxygen concentration. When the 661W cell line reached 80% confluence, the cells were then incubated in OGD solution with 5 μM zinc for 3 or 6 hours and observed under a fluorescence microscope and MMP Zymogram.

Assessment of Cell Death

Cell death caused by zinc accumulation was quantified by measuring lactate dehydrogenase (LDH) activity released into the culture medium.[19] LDH activity was estimated by measuring the rate of decrease in absorbance at 340 nm, using an automated microplate reader (UVmax; Molecular Devices, San Francisco, CA, USA). After subtracting background (sham-washed control cultures), LDH values were normalized to the mean maximal value (defined as 100%) in parallel cultures exposed to 400 μM $ZnCl_2$ for 24 hours, conditions that caused complete cell death.

Measurement of Cell Viability

MTT assay was used to determine the degree of apoptosis in 661W cells. Since LDH activities were not detected in 661W cells, zinc-treated cell death was confirmed by using MTT assays in 661W cells. After the experiment, medium was removed and the MTT solution was exposed to 661W cells for 1 hour at 37°C. MTT assay was estimated by using an automated microplate reader (UVmax) at an absorbance of 590 nm.

Statistical Analysis

All results are presented as means ± SEM. Student's *t*-tests were used to evaluate the significance of difference between two groups. When there were more than two experimental groups, we performed 1-way ANOVA with Bonferroni correction. P values < 0.05 were considered significant. All statistical analyses and graphical presentations were conducted and created with Sigma Plot version 10.0 software (Systat Software, Inc., San Jose, CA, USA).

RESULTS

Establishment of Experimental RD in Mice

A mouse model of RD was established by subretinal injection of 1:1 mixture of BSS and Healon as described in Methods. Formation of reproducible bullous RD was confirmed by fundus photographs, using the Micron III retinal imaging system. Histologic sections stained with H&E revealed separation of the retina proper from the RPE (Fig. 1, arrows).

Photoreceptor Cell Apoptosis After RD in Mice

We observed cell death by RD over time. TUNEL staining revealed conspicuous photoreceptor cell death in the center of the detachment area beginning on day 1 post RD; no staining was seen in other retinal layers. TUNEL staining of photoreceptor cells appeared to peak on day 3 post RD, at which point these cells covered the entire extent of the detached area (Fig. 2A).[20] On the basis of these observations, we chose day 3 post RD as the standard time point for evaluating TUNEL-based cell death. No TUNEL-labeled cells were found in the control retinas.

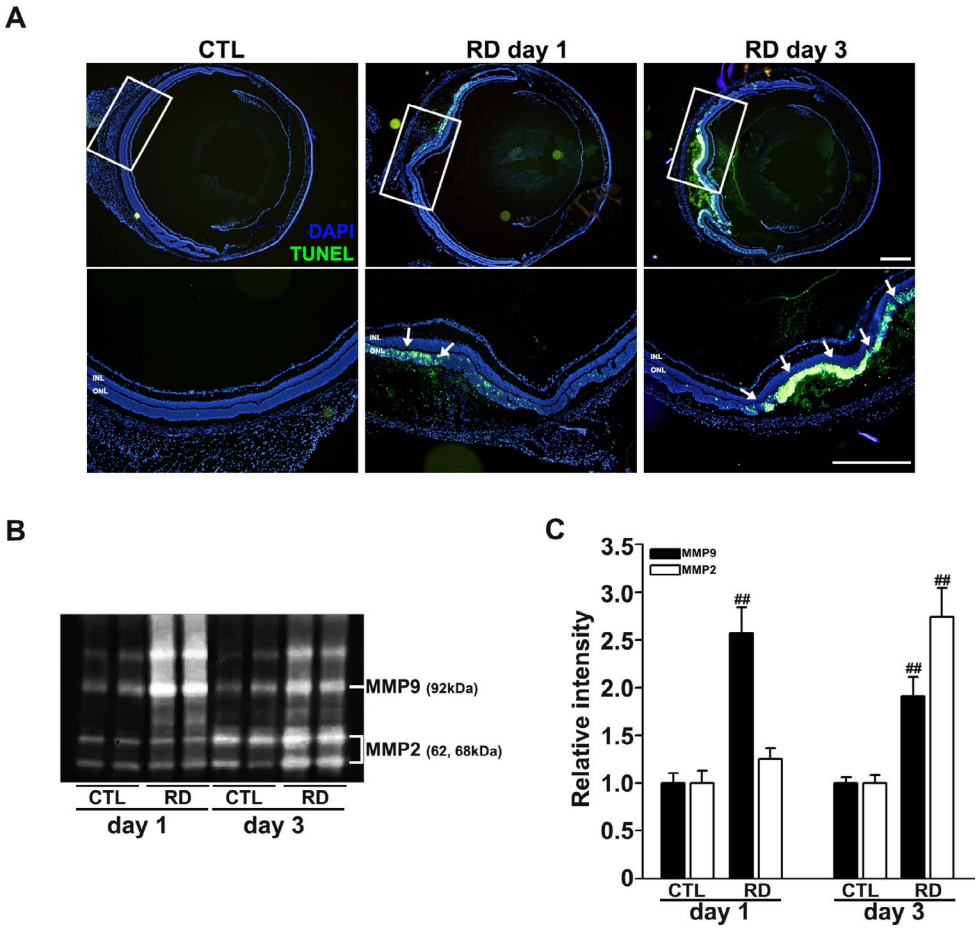

FIGURE 2. MMP activation and photoreceptor cell death in RD mice retinal tissue. (**A**) Representative fluorescence photomicrographs of TUNEL (*green*)–labeled retinal tissues under control conditions and on days 1 and 3 post RD. Scattered TUNEL-positive cells (*arrows*) appeared in the photoreceptor layer of the detached retina on day 1 post RD. The number of TUNEL-positive photoreceptor cells was markedly increased on day 3 post RD. Nuclei were stained with DAPI (*blue*). Portions of the retina denoted by *squares* in the *upper panel* (original magnification, ×40) are magnified in the images in the *lower panel* (original magnification, ×100); *scale bar*: 500 μm. (**B**) MMP zymography on gelatin gels. Zymograms showed that MMP-2 and MMP-9 activity were increased in retinal tissues after RD formation. MMP-9 activity was markedly increased 1 day after RD, whereas MMP-2 activity was increased 3 days after RD; activity of the active form of MMP-2 was more markedly increased. (**C**) Quantification of MMP zymography on gelatin gels. *Bars* denote densitometric measurements (means ± SEM; $n = 9$ each) of gelatin MMP-activated bands, normalized to the mean of the respective control (CTL), defined as 1. $##P < 0.001$ compared with respective CTL values on days 1 and 3.

Activation of Matrix Metalloproteinase in RD Mice

We next examined MMP-2 and MMP-9 activity in retinal tissues from control and RD mice. Gel zymography showed that the gelatinolytic activities of pro and active forms of MMP-2 and MMP-9 were significantly elevated in the RD group (Fig. 2B, Supplementary Fig. S1). A densitometric analysis of MMP gel zymograms revealed that MMP-9 activity was markedly increased on day 1 post RD, followed by a substantial decrease day 3 post RD. MMP-2 activity was increased at a slower rate than that of MMP-9; activities of both pro and active forms of MMP-2 remained unchanged on day 1, but the activity of the active form was substantially elevated on day 3 post RD (Fig. 2C). Consistent with the temporal pattern of TUNEL staining corresponding to photoreceptor cell death, MMP activity gradually declined thereafter.

Evidence for Retinal Hypoxia After RD

Diverse mechanisms have been proposed to account for photoreceptor cell death in RD, one of which is hypoxia.[21,22] To examine this possibility, we assessed the hypoxic state of photoreceptor cells in RD by staining retinal flat mounts prepared from control and RD mice, using a pimonidazole-based Hypoxyprobe kit on days 1 and 3 post RD. Confocal microscopy showed that pimonidazole-positive hypoxic cells began to appear on day 1 post RD, scattered within the area of detachment. On day 3 post RD, the number of hypoxic cells substantially increased to cover the entire detachment area (Fig. 3A). A series of z-stack confocal microscopy images showed that most pimonidazole-positive hypoxic cells were concentrated in the outer retinal layer, indicating that hypoxia/hypoperfusion in RD occurs predominantly in this deep layer where photoreceptor cells reside (Fig. 3B).

Zinc Accumulation in Degenerating Photoreceptor Cells of RD Model Mice

To evaluate changes in intracellular free zinc levels after RD, we collected eyeballs at the indicated time points (1 and 3 days post RD) and stained retinal sections with the zinc-specific fluorescent dye TFL-Zn. In control retinas, free or labile zinc appeared to be enriched in photoreceptor outer segments and in the inner nuclear and ganglion cell layers (Fig. 4A). On day 1 post RD, overall zinc staining pattern in the retina after RD

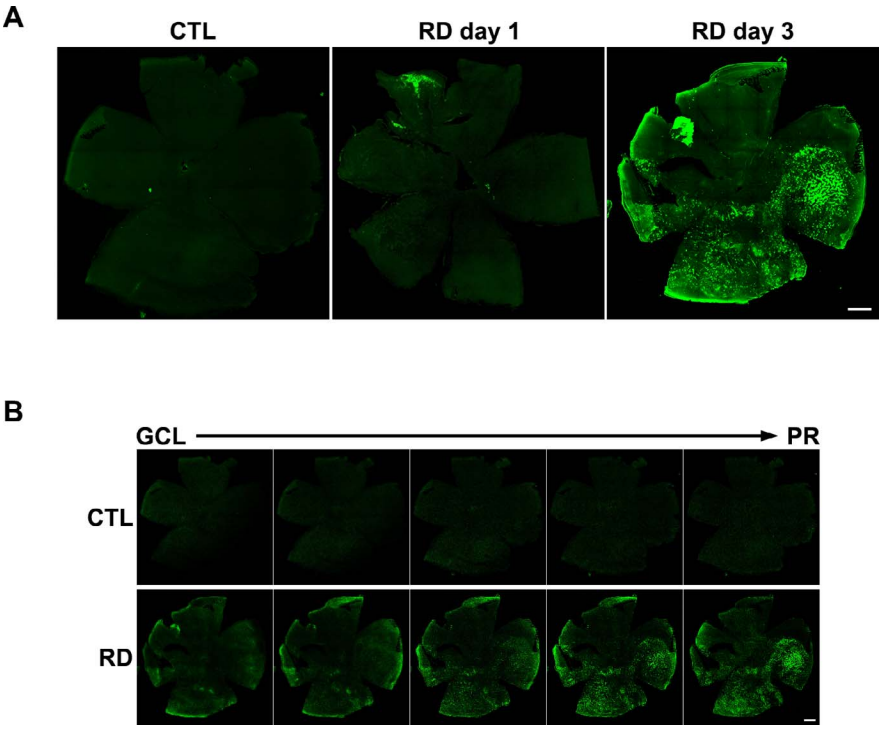

FIGURE 3. Evidence for hypoxia in detached retinas. (**A**) Fluorescence photomicrographs of control, day 1, and day 3 post-RD retinal flat mounts stained by using the Hypoxyprobe method. The small number of hypoxyprobe-positive cells was noted on day 1, but both the number of such cells and their staining intensity were substantially increased on day 3. Images shown are representative of six experiments; *scale bar*: 500 μm. (**B**) Representative series of z-stack confocal microscopy images of the tissues shown in (**A**). Hypoxyprobe-positive cells are concentrated in the deep layer where photoreceptor cells reside, indicating that this layer may be exposed to more severe hypoxia/ischemia after RD. *Scale bar*: 500 μm. CTL, controls; GCL, ganglion cell layer; PR, photoreceptor.

changed over time, indicating a decrease in free zinc levels of the retina. On the other hand, a few scattered photoreceptor cell bodies began to exhibit TFL-Zn fluorescence, especially in the photoreceptor outer segment, indicating an increase in free zinc levels. On day 3 post RD, the number of intensely TFL-Zn–positive dots (zinc accumulation) was significantly increased in the photoreceptor cell layer including outer segments (Fig. 4B). The staining pattern in extraocular connective tissue remained relatively unchanged regardless of time points. Such a temporal pattern matched well with that of TUNEL staining. Upon observing this phenomenon, we speculated that zinc in retinal tissue is depleted when the retina becomes ischemic upon detachment from the RPE, and that zinc accumulates afterwards upon cellular death.

Because TFL-Zn stains only labile or free zinc, which constitutes only a fraction of total zinc, increases in zinc staining may reflect changes in the binding status of zinc in the absence of changes in total zinc levels. To address this possibility, we measured the total amount of zinc in retinal tissue with a zinc assay kit (Metallogenics). These analyses showed that the relative amount of total zinc in RD mouse eyes (37.71 ± 1.98 μg/dL) was not significantly different from that in corresponding control eyes (42.37 ± 1.83 μg/dL, $P > 0.05$) on day 1 post RD (Fig. 4C). Although the relative amount of total zinc in the entire eyeball on day 3 trended higher in RD eyes (53.98 ± 5.19 μg/dL) than in the corresponding control eyes (45.08 ± 6.08 μg/dL), this difference was not statistically significant ($P > 0.05$), even though there was a marked accumulation of free zinc in retinal photoreceptor cells at this time. To further dissect the effect of RD on the total amount of zinc, we divided eyeballs into two parts: RD involved and RD uninvolved. The RD-involved part showed a significantly higher relative zinc concentration (40.79 ± 5.09 μg/dL) than the RD-uninvolved part (23.03 ± 2.40 μg/dL, $P < 0.05$) or the corresponding control eyes (25.08 ± 4.36 μg/dL, $P < 0.05$) on day 3 post RD (Fig. 4D). Hence, the accumulation of free zinc in photoreceptor cells of RD mice detected with TFL-Zn staining correlated well with the increase in total zinc levels.

Increases in Intracellular Zinc Levels Enhance Hypoxyprobe Staining and MMP Activation in Response to Oxygen-Glucose Deprivation in Cultured Retinal Cells and Photoreceptor-Derived 661W Cells

To determine the relationship between hypoxia and increases in intracellular free zinc, we exposed primary retinal cell cultures and 661W photoreceptor cell cultures to OGD conditions for 3 hours to induce ischemia. Treatment of primary retina cells with 5 μM zinc increased the activity of MMP-9 compared with that in OGD-alone or normoxia controls (Figs. 5A, 5B). Immunocytochemistry confirmed that exposure of 661W cells to OGD and zinc increased the number of Hypoxyprobe-stained hypoxic cells and intensity of staining to a greater degree than exposure to OGD alone did (Fig. 5C). Exposure to zinc alone did not increase hypoxia, when compared with sham-washed controls, as evidenced by negative Hypoxyprobe staining. Taken together, these results suggest that zinc dyshomeostasis potentiates hypoxia-induced changes in photoreceptor cells.

Attenuation of Photoreceptor Cell Death in RD Mice by Chelation of Extracellular Zinc

To identify a possible role of zinc in MMP activation and photoreceptor cell death in RD, we experimentally reduced

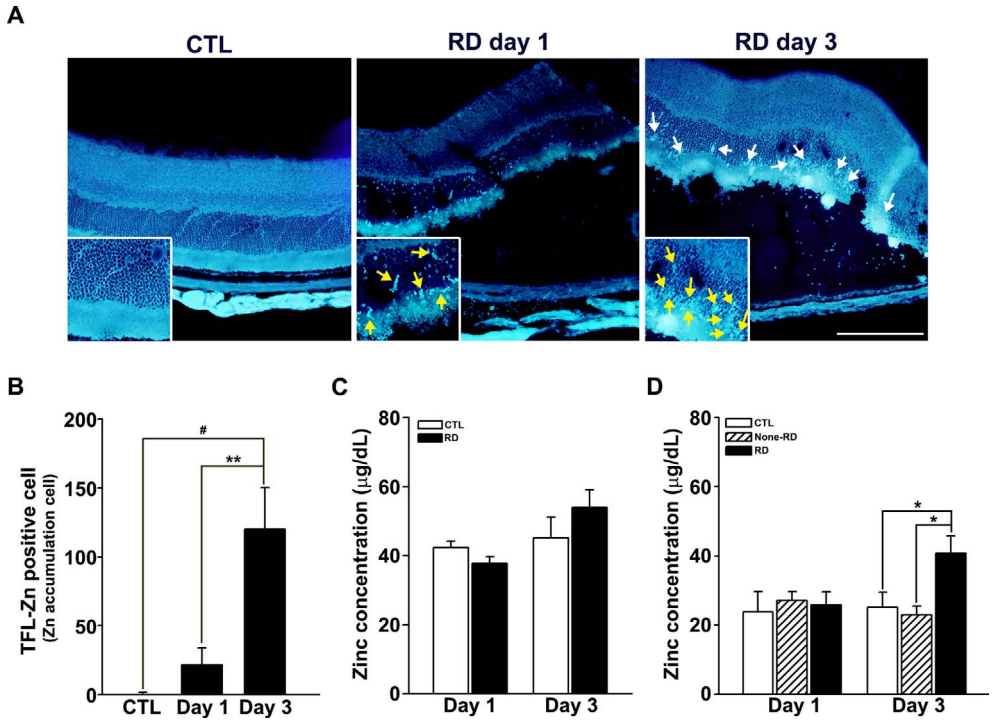

FIGURE 4. Zinc accumulation in photoreceptor cells of RD mice retinal tissue. (**A**) Retinal tissues stained with TFL-Zn, a zinc-sensitive fluorescent dye. Zinc fluorescence appeared to decrease in the retina 1 day after RD, especially in the outer segment (*arrows*), compared with controls (CTL). After 3 days, in contrast, intense zinc fluorescence was observed in photoreceptor cell bodies in the detached retina. Original magnification, ×200; *scale bar*: 200 μm. (**B**) Quantification of TFL-Zn–positive dots, which denote zinc accumulation in photoreceptor cell layer. TFL-Zn–positive dots were significantly increased on day 3 post RD, which means an increase of free zinc level in photoreceptor cells on day 3 post RD ($n = 5$–6). (**C**) Quantification of total zinc concentration in whole retinal tissue. *Bars* denote concentrations of total (bound and free) zinc in whole control retinas or RD retinas 1 and 3 days after RD ($n = 16$–20). Although there was a tendency toward an increase on day 3 in RD samples, the difference was not significant ($P > 0.05$). (**D**) Quantification of total zinc concentration in half retinal tissue. *Bars* denote concentrations of total zinc in a retina half, with and without RD, on day 1 and day 3 post RD. Zinc concentration was not different from control, non-RD, and RD retinas on day 1 post RD, but total zinc level was markedly increased on day 3 in the RD-containing region of retinal tissue compared with the non-RD region or control ($n = 10$–16, $^*P < 0.05$).

zinc concentrations in the subretinal space by using the extracellular zinc-chelator CaEDTA (500 μM), added to a mixture of BSS and Healon at the time of RD formation. Compared with normal-RD, CaEDTA-treated RD exhibited marked decreases in MMP activity (Figs. 6A, 6B) and Zn-accumulating TFL-Zn–positive dots in the photoreceptor cell layer (Fig. 6C) on day 3 post RD. Upon chelation of extracellular zinc, in addition, both TUNEL-positive photoreceptor cells and hypoxyprobe-positive retinal cells were reduced (Figs. 6D, 6E). These results suggest that release of zinc into the subretinal space is a key contributing factor to MMP activation and may potentiate hypoxia-induced photoreceptor cell death by causing subsequent zinc dyshomeostasis.

Reduced Photoreceptor Cell Death by Inhibition of MMP in RD Mice

The preceding results indicate that zinc dyshomeostasis, probably triggered by hypoxia/ischemia-induced zinc movement in the deep layer of the retina, contributes to MMP activation and photoreceptor cell death in RD. In the next set of experiments, we examined the role of MMPs in RD-induced photoreceptor cell death. To reduce MMP activation in RD, we administered GM6001 or minocycline (1 mM), mixed in 3 μL of the fluid injected into the subretinal space at the time of RD formation, followed by daily intraperitoneal injection of GM6001 (10 mg/kg) or minocycline (50 mg/kg) once a day for 3 days. Gelatin gel zymography showed that treatment with GM6001 or minocycline almost completely blocked increases in MMP-2 and MMP-9 activity in RD mice on day 3 post RD (Figs. 7A, 7B). To assess photoreceptor cell death in these experiments, we stained retinas by using the TUNEL method. Treatment with GM6001 or minocycline significantly reduced the number of TUNEL-positive dots in the photoreceptor cell layer (Figs. 7C, 7D).

Using primary retinal cells in culture, we tested whether the cell death induced by zinc dyshomeostasis was also mediated by MMP activation. Cell death was quantified by measuring LDH release from dead cells after 24 hours of continuous exposure to zinc. Exposure to 70 μM zinc resulted in 80% cell death, whereas addition of 0.1 or 1 μM minocycline or GM6001 markedly reduced zinc-induced cell death in these cultures, decreasing it by approximately 60% (Figs. 7E, 7F). Also, we observed the same patterns in 661W cells. Cell viability was increased in 50 or 100 μM minocycline- or GM6001-treated 661W cells compared with 50 μM zinc-treated 661W cells (Figs. 7G, 7H). The results demonstrated the role of MMPs in modulation of zinc-induced cell death.

DISCUSSION

To our knowledge, this is the first study to show that zinc dyshomeostasis occurs in RD and plays a critical role in associated MMP activation and photoreceptor cell death. It is well established that zinc dyshomeostasis contributes to neuronal cell death in many acute brain injury settings.[23–25]

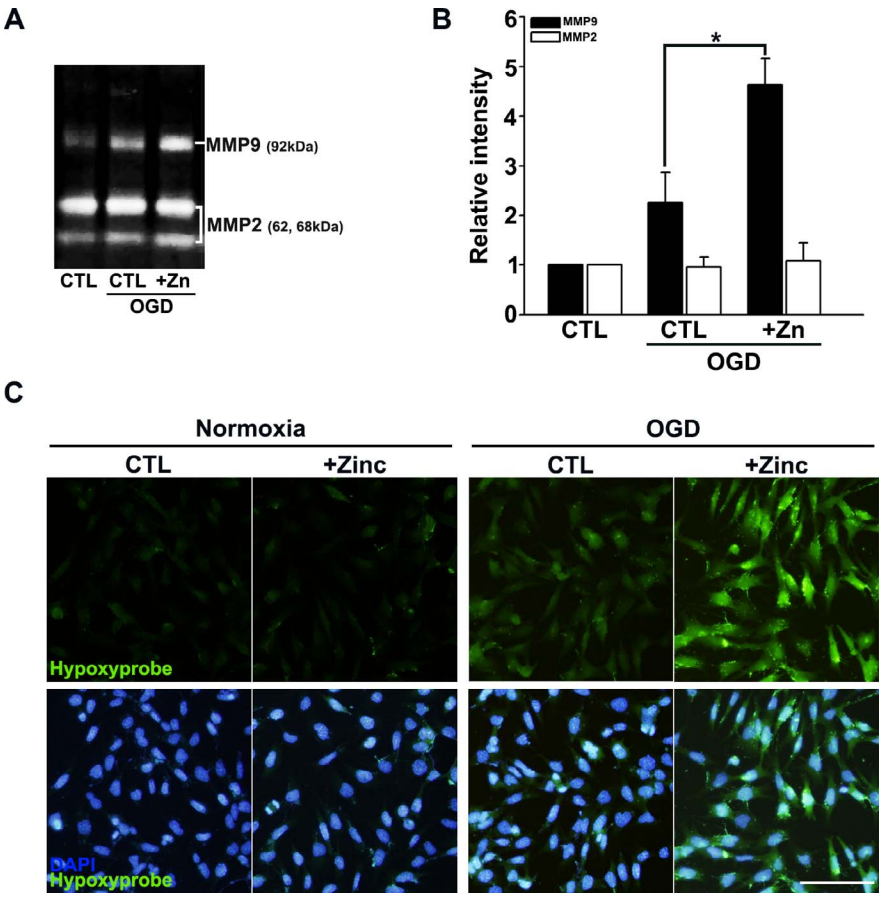

Figure 5. Relationship of zinc to MMP activation and hypoxia in primary retinal cells and 661W cells. (**A**) Representative gelatin gel zymogram. Cultures of primary retinal cells were exposed to combined OGD conditions for 3 hours. MMP-9 activity was increased in treatment with 5 μM zinc during OGD compared with OGD alone. MMP-2 activity was little changed. (**B**) Quantification of MMP zymography. *Bars* denote densitometric measurements (means ± SEM, $n = 3$) of the MMP bands shown in MMP zymography gel (normalized to the mean of the respective control, defined as 1). (**C**) Hypoxyprobe-stained images in 661W cells. 661W cells were exposed to OGD or OGD with 5 μM zinc, and stained by using the Hypoxyprobe method. Nuclei were stained with DAPI (*blue*). As expected, hypoxic cells were increased when zinc was cotreated with OGD compared with OGD alone. However, normoxia or normoxia with 5 μM zinc has no effect on hypoxic cells. Original magnification, ×200; *scale bar*: 200 μm.

From a mechanistic standpoint, studies have suggested that mitochondrial and lysosomal damage, oxidative stress, poly [ADP-ribose] polymerase (PARP) activation, and energy depletion may contribute to the cytotoxicity of zinc dyshomeostasis.[26,27]

One interesting finding of the present study was that RD causes a reduction in free zinc levels in the retina, particularly in the outer segment, an event that is followed by substantial increases in free zinc levels in photoreceptor cell bodies. Two possible mechanisms can be invoked to explain this finding. In the first, which involves purely intracellular events, free zinc may be sequestered initially (bound to proteins or absorbed by organelles, and thus inaccessible to TFL-Zn staining) and then is relocated to cell bodies of photoreceptors again as free zinc. The second involves extracellular zinc release and reuptake, as well as additional zinc influx. As is the case in brain ischemia,[24] zinc accumulation in photoreceptor cells and subsequent photoreceptor cell death in RD were both attenuated by injection of the extracellular zinc-chelator CaEDTA into the subretinal space. These results support the second possibility and may mean that the increase in zinc in the extracellular space is a prerequisite for the subsequent zinc accumulation in photoreceptor cells and their death.

In terms of the mechanism of extracellular zinc release, it is possible that ischemia plays a key role, given that separation of the neural retina from the underlying choroidal vasculature has been reported to create an ischemic environment in the outer retina.[28–30] In support of this scenario, we found that the Hypoxyprobe predominantly stained photoreceptor cells in the RD area, largely sparing other retinal neurons. Neuronal depolarization following ischemia may induce zinc release into the extracellular space, often concomitantly with glutamate release.[31] In the central nervous system, including the retina, such zinc release may contribute to subsequent zinc accumulation and death of neurons.[14,23,24] In addition, Zn dyshomeostasis affected Hypoxyprobe staining (Fig. 5). Although it is unknown how zinc dyshomeostasis increases Hypoxyprobe staining, it is well established that it can cause increases in reactive oxygen species (ROS) in cells.[32] Direct consumption of oxygen in making ROS or indirect effects of ROS, such as ATP depletion,[33] might contribute to compensatory mitochondrial oxygen consumption and hence lower oxygen levels. Further studies may be needed to address this issue.

Although ischemia likely plays a large role in extracellular zinc release, other mechanisms may exist to explain the early depletion of zinc in the retina following RD. For example, structural damage to the outer segment can disrupt phototransduction in photoreceptors; this process may involve dynamic changes in free zinc inside photoreceptors, as exemplified by the light-dependent movement of free zinc

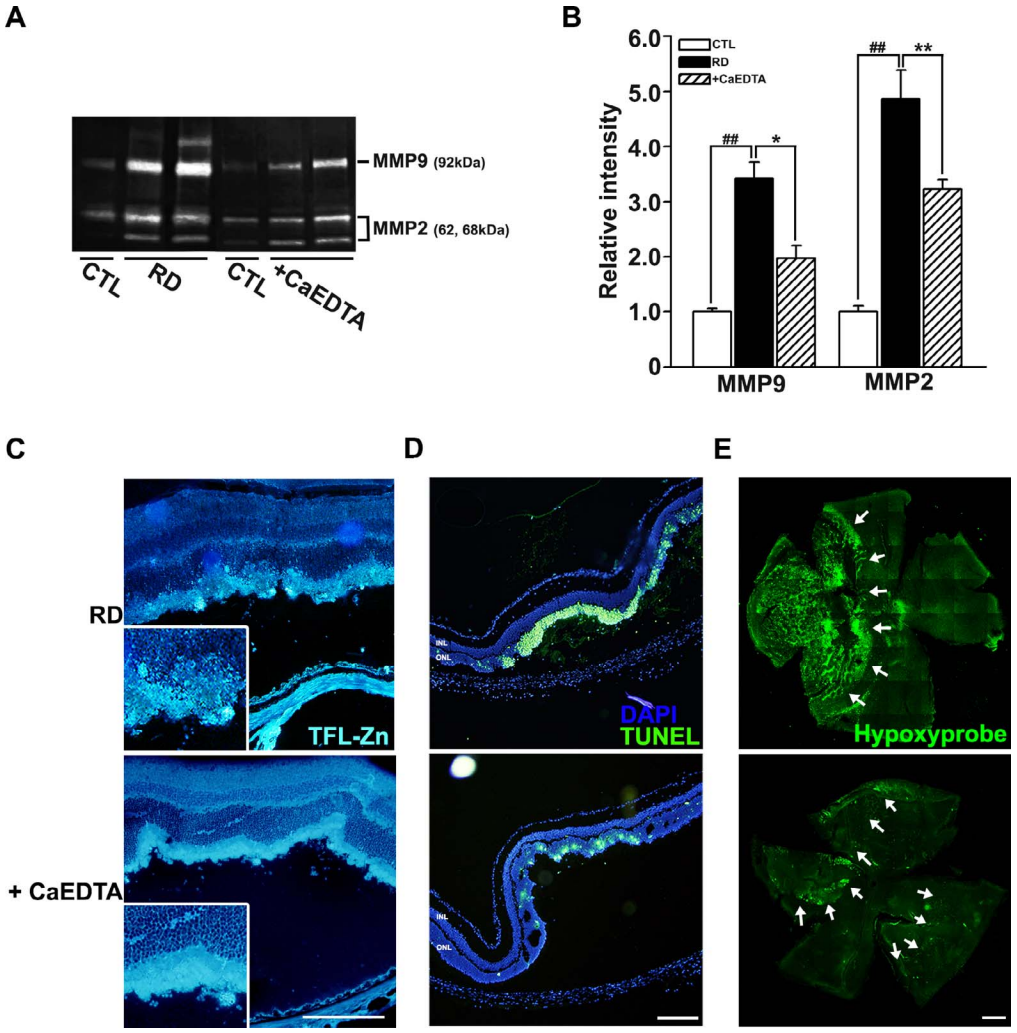

Figure 6. Attenuation of photoreceptor cell death in RD mice by chelation of extracellular zinc. (**A**) Representative gelatin gel zymogram. RD increased MMP-2 and -9 activity. Injection of 500 μM CaEDTA into the subretinal space attenuated the increase in MMP-2 and MMP-9 activity in RD mice 3 days post RD. (**B**) Quantification of MMP zymography. *Bars* denote densitometric measurements (means ± SEM, $n = 3$–6) of the gelatin MMP zymogram bands shown in (**A**) (normalized to the mean of the respective control, defined as 1). $^{*}P < 0.05$, $^{**}P < 0.01$, $^{\#\#}P < 0.001$. (**C**) Retinal tissues stained with TFL-Zn, a zinc-sensitive fluorescent dye. Zinc accumulation was decreased in CaEDTA-treated retinas ($n = 6$) compared with RD-only retinas ($n = 3$) on day 3 post RD. Original magnification, ×200; *scale bar*: 200 μm. (**D**) Representative fluorescence photomicrographs of TUNEL-stained retinal tissue sections. Intense TUNEL fluorescence was detected in photoreceptor cell bodies following RD ($n = 3$), but was markedly reduced by treatment with CaEDTA ($n = 6$). Original magnification, ×100; *scale bar*: 200 μm. (**E**) Flat-mount images of Hypoxyprobe-stained retinas after RD-only or RD-plus-CaEDTA treatment. Compared with RD alone ($n = 3$), the number of hypoxic cells was markedly reduced in CaEDTA-treated retinas ($n = 6$). *Scale bar*: 500 μm.

between rods/cones and cell bodies in photoreceptor cells.[13,34,35] Hence, it is conceivable that such intracellular relocation of free zinc could at least partly underlie the initial depletion of zinc in the outer segment and late increase in cell bodies of photoreceptor cells. However, the finding that CaEDTA, an extracellular zinc chelator, prevented the late accumulation of zinc in cell bodies argues against this possibility. Moreover, the amount of total zinc was increased in RD (Fig. 4D), further supporting the possibility that additional zinc had to have come from outside. The origin of the extra zinc that accumulates in degenerating photoreceptor cells is unknown, but blood, which contains very high levels of zinc, would seem to be a plausible source.[36]

Deregulated MMP activity is a common characteristic of many diseases, including neurodegenerative disorders.[37] Moreover, MMPs in the retina have been linked to pathologic processes that involve matrix degradation, cell proliferation, neovascularization, and inflammation.[10,38,39] Our current results indicate that MMP-2 and MMP-9 were activated in experimental RD, yet with different time courses. Even on day 1 post RD, the activity of MMP-9 increased by 2.5-fold. On day 3 post RD, MMP-2 and MMP-9 activity were found to have increased. And, there was some variability in MMP-2 and MMP-9 fold increases in different experimental sets, which might depend on the baseline level of each MMP. Our data suggest that an overall increase in MMP activity, and not an increase in the activity of a specific MMP, may be responsible for the present results. In this regard it is noteworthy that substrate specificity of MMP-2 and MMP-9 overlaps substantially. To determine which MMP plays a more important role herein, further studies using selective inhibitors (not available) or antisense strategy might be necessary.

Since activity-dependent release of extracellular zinc leads to MMP activation in cultured cortical neurons,[40] ischemia-triggered zinc release into the extracellular space might contribute to the activation of MMP-9 in RD. Whether late

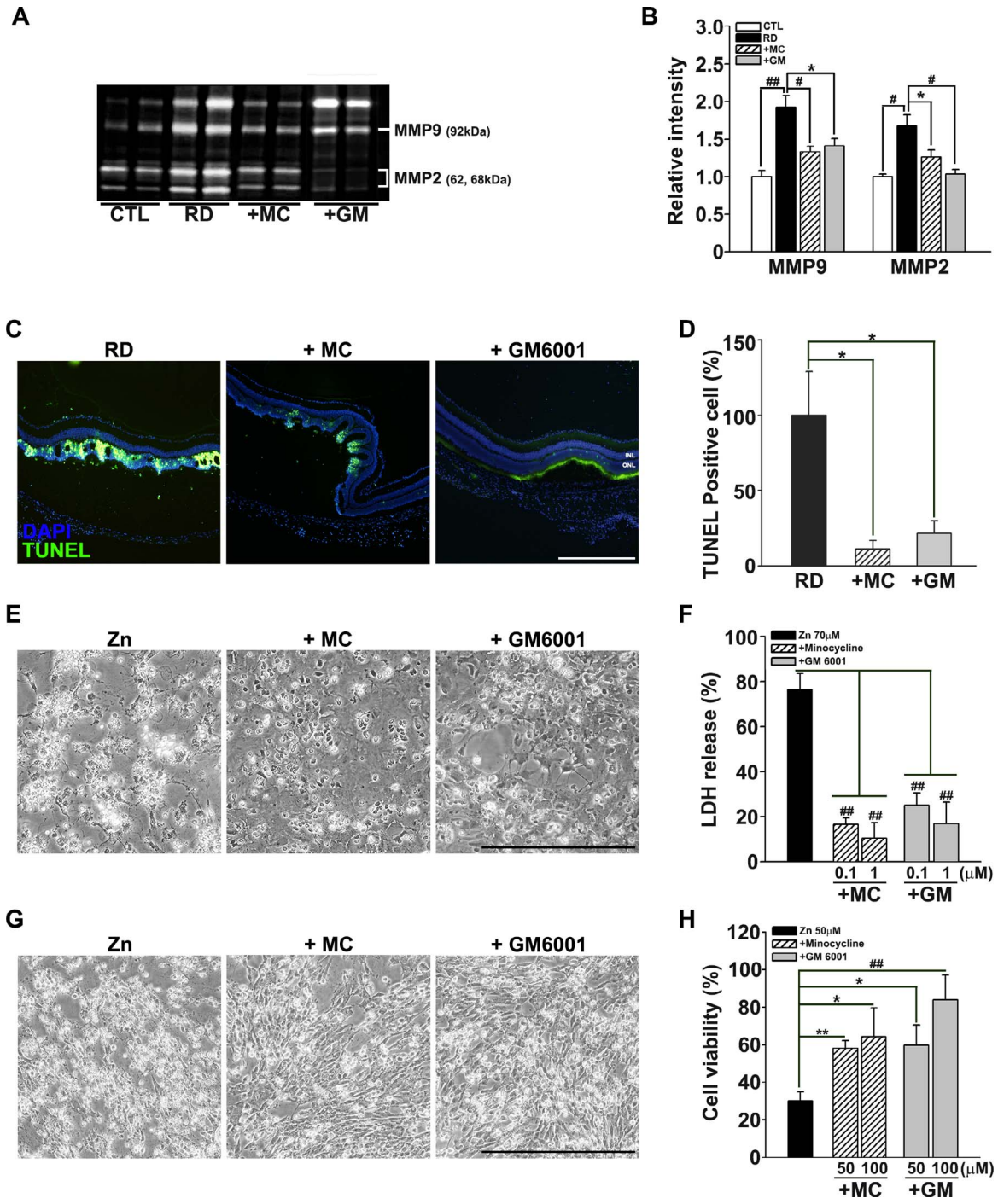

Figure 7. Reduction in photoreceptor cell death in RD mice by inhibition of MMPs. (**A**) Gelatin MMP zymography. MMP-9 and MMP-2 activity were markedly upregulated following RD. Addition of minocycline (MC, 50 mg/kg; $n = 12$) or GM6001 (GM, 10 mg/kg; $n = 10$) markedly attenuated RD-induced increases in MMP activity. $^{*}P < 0.05$, $^{\#}P < 0.005$, $^{\#\#}P < 0.001$. (**B**) Quantification of MMP zymography. *Bars* denote densitometric measurements (means ± SEM, $n = 7$–12) of the gelatin MMP-9 and -2 bands shown in zymography gels (normalized to the mean of the respective control, defined as 1). (**C**) Representative TUNEL staining image of retinas and (**D**) quantification of number of TUNEL-positive photoreceptor cells on day 3 post RD. Nuclei were stained with DAPI (*blue*). TUNEL-positive (*green*) photoreceptor cells were significantly decreased with treatment of minocycline or GM6001 as compared with those of RD ($n = 4$–5). $^{*}P < 0.05$; original magnification, ×100; *scale bar*: 500 μm. (**E**) Representative photomicrographs of retinal cultures and (**F**) quantification of LDH release. Retinal cells were exposed to 70 μM zinc, zinc plus 0.1 or 1 μM minocycline, or zinc plus 0.1 or 1 μM GM6001 for 24 hours. Minocycline or GM6001 treatment has protective effect on zinc-treated cell death ($n = 4$). $^{\#\#}P < 0.001$; original magnification, ×200; *scale bar*: 500 μm. (**G**) Representative photomicrographs of 661W cells and (**H**) quantification of MTT assay. 661W cells were exposed to 50 μM zinc, zinc plus 50 or 100 μM minocycline, or zinc plus 50 or 100 μM GM6001 for 24 hours. Cell viability was increased in minocycline- or GM6001-treated cells compared with zinc-treated cells ($n = 4$–5). $^{*}P < 0.05$, $^{**}P < 0.01$, $^{\#\#}P < 0.001$; original magnification, ×200; *scale bar*: 500 μm. CTL, controls.

zinc accumulation is responsible for MMP-2 activation is unknown, but consistent with this possibility, zinc dyshomeostasis combined with OGD in vitro selectively increased MMP-9 (Fig. 5). Our demonstration that the MMP inhibitors GM6001 and minocycline attenuated zinc-induced in vivo photoreceptor cell death in RD, as well as in vitro cultured retinal cell and 661W cell death, support the hypothesis that MMP activation is a significant contributor to zinc dyshomeostasis–related photoreceptor cell death in RD. In addition, these findings are in line with the existing literature, which shows that activation of MMP-9 in RD leads to retinal cell death by interfering with integrin-mediated survival signaling.[38,41] Müller cells in the retina have been considered the main source of MMPs,[42–44] and MMP-2 and MMP-9 are also found in microglia and degenerating retinal ganglion cells.[45]

In conclusion, the present study demonstrated the novel finding that, following experimental RD in mice, free zinc accumulates in degenerating photoreceptor cell bodies, which also exhibit evidence of having received hypoxic insults. Our results provide evidence that such hypoxia-triggered zinc dyshomeostasis may underlie MMP activation in and around photoreceptor cells, and that activated MMPs play a causal role in the death of these cells. Blocking zinc dyshomeostasis with chelators or pyruvate, or inhibiting MMPs during the early stage of RD, may prove effective in reducing photoreceptor cell death and thus preserving vision after RD.

Acknowledgments

Supported by grants from the Ministry of Science, ICT and Future Planning, Republic of Korea (NRF-2017R1D1A1B05028221) and the Asan Institute for Life Sciences, Asan Medical Center, Seoul, Republic of Korea (2017-084, 2018-084).

Disclosure: **J. Choi**, None; **Y.J. Kim**, None; **B.-R. Seo**, None; **J.-Y. Koh**, None; **Y.H. Yoon**, None

References

1. Arroyo JG, Yang L, Bula D, Chen DF. Photoreceptor apoptosis in human retinal detachment. *Am J Ophthalmol*. 2005;139:605–610.
2. Hisatomi T, Sakamoto T, Goto Y, et al. Critical role of photoreceptor apoptosis in functional damage after retinal detachment. *Curr Eye Res*. 2002;24:161–172.
3. Cook B, Lewis GP, Fisher SK, Adler R. Apoptotic photoreceptor degeneration in experimental retinal detachment. *Invest Ophthalmol Vis Sci*. 1995;36:990–996.
4. Chinskey ND, Zheng QD, Zacks DN. Control of photoreceptor autophagy after retinal detachment: the switch from survival to death. *Invest Ophthalmol Vis Sci*. 2014;55:688–695.
5. Mantopoulos D, Murakami Y, Comander J, et al. Tauroursodeoxycholic acid (TUDCA) protects photoreceptors from cell death after experimental retinal detachment. *PLoS One*. 2011;6:e24245.
6. Liu H, Qian J, Wang F, et al. Expression of two endoplasmic reticulum stress markers, GRP78 and GADD153, in rat retinal detachment model and its implication. *Eye (Lond)*. 2010;24:137–144.
7. Zhu H, Qian J, Wang W, et al. RNA interference of GADD153 protects photoreceptors from endoplasmic reticulum stress-mediated apoptosis after retinal detachment. *PLoS One*. 2013;8:e59339.
8. Nakazawa T, Takeda M, Lewis GP, et al. Attenuated glial reactions and photoreceptor degeneration after retinal detachment in mice deficient in glial fibrillary acidic protein and vimentin. *Invest Ophthalmol Vis Sci*. 2007;48:2760–2768.
9. Gonzalez-Avila G, Mendez D, Lozano D, Ramos C, Delgado J, Iturria C. Role of retinal detachment subretinal fluid on extracellular matrix metabolism. *Ophthalmologica*. 2004;218:49–56.
10. Sivak JM, Fini ME. MMPs in the eye: emerging roles for matrix metalloproteinases in ocular physiology. *Prog Retin Eye Res*. 2002;21:1–14.
11. Klein T, Bischoff R. Physiology and pathophysiology of matrix metalloproteases. *Amino Acids*. 2011;41:271–290.
12. Miceli MV, Tate DJ Jr, Alcock NW, Newsome DA. Zinc deficiency and oxidative stress in the retina of pigmented rats. *Invest Ophthalmol Vis Sci*. 1999;40:1238–1244.
13. Akagi T, Kaneda M, Ishii K, Hashikawa T. Differential subcellular localization of zinc in the rat retina. *J Histochem Cytochem*. 2001;49:87–96.
14. Yoo MH, Lee JY, Lee SE, Koh JY, Yoon YH. Protection by pyruvate of rat retinal cells against zinc toxicity in vitro, and pressure-induced ischemia in vivo. *Invest Ophthalmol Vis Sci*. 2004;45:1523–1530.
15. Matsumoto H, Kataoka K, Tsoka P, Connor KM, Miller JW, Vavvas DG. Strain difference in photoreceptor cell death after retinal detachment in mice. *Invest Ophthalmol Vis Sci*. 2014;55:4165–4174.
16. Matsumoto H, Miller JW, Vavvas DG. Retinal detachment model in rodents by subretinal injection of sodium hyaluronate. *J Vis Exp*. 2013;79:50660.
17. Kim TY, Yi JS, Chung SJ, et al. Pyruvate protects against kainate-induced epileptic brain damage in rats. *Exp Neurol*. 2007;208:159–167.
18. Yoon YH, Jeong KH, Shim MJ, Koh JY. High vulnerability of GABA-immunoreactive neurons to kainate in rat retinal cultures: correlation with the kainate-stimulated cobalt uptake. *Brain Res*. 1999;823:33–41.
19. Koh JY, Choi DW. Quantitative determination of glutamate mediated cortical neuronal injury in cell culture by lactate dehydrogenase efflux assay. *J Neurosci Methods*. 1987;20:83–90.
20. Yang L, Bula D, Arroyo JG, Chen DF. Preventing retinal detachment-associated photoreceptor cell loss in Bax-deficient mice. *Invest Ophthalmol Vis Sci*. 2004;45:648–654.
21. Liu H, Zhu H, Li T, Zhang P, Wang N, Sun X. Prolyl-4-hydroxylases inhibitor stabilizes HIF-1alpha and increases mitophagy to reduce cell death after experimental retinal detachment. *Invest Ophthalmol Vis Sci*. 2016;57:1807–1815.
22. Shelby SJ, Angadi PS, Zheng QD, Yao J, Jia L, Zacks DN. Hypoxia inducible factor 1alpha contributes to regulation of autophagy in retinal detachment. *Exp Eye Res*. 2015;137:84–93.
23. Choi DW, Koh JY. Zinc and brain injury. *Annu Rev Neurosci*. 1998;21:347–375.
24. Koh JY, Suh SW, Gwag BJ, He YY, Hsu CY, Choi DW. The role of zinc in selective neuronal death after transient global cerebral ischemia. *Science*. 1996;272:1013–1016.
25. Capasso M, Jeng JM, Malavolta M, Mocchegiani E, Sensi SL. Zinc dyshomeostasis: a key modulator of neuronal injury [discussion in *J Alzheimers Dis*. 2005;8:209–215]. *J Alzheimers Dis*. 2005;8:93–108.
26. Lee SJ, Koh JY. Roles of zinc and metallothionein-3 in oxidative stress-induced lysosomal dysfunction, cell death, and autophagy in neurons and astrocytes. *Mol Brain*. 2010;3:30.
27. Sensi SL, Paoletti P, Koh JY, Aizenman E, Bush AI, Hershfinkel M. The neurophysiology and pathology of brain zinc. *J Neurosci*. 2011;31:16076–16085.
28. Bertram KM, Bula DV, Pulido JS, et al. Amino-acid levels in subretinal and vitreous fluid of patients with retinal detachment. *Eye (Lond)*. 2008;22:582–589.

29. Mervin K, Valter K, Maslim J, Lewis G, Fisher S, Stone J. Limiting photoreceptor death and deconstruction during experimental retinal detachment: the value of oxygen supplementation. *Am J Ophthalmol*. 1999;128:155–164.
30. Lewis G, Mervin K, Valter K, et al. Limiting the proliferation and reactivity of retinal Müller cells during experimental retinal detachment: the value of oxygen supplementation. *Am J Ophthalmol*. 1999;128:165–172.
31. Galasso SL, Dyck RH. The role of zinc in cerebral ischemia. *Mol Med*. 2007;13:380–387.
32. Kim EY, Koh JY, Kim YH, Sohn S, Joe E, Gwag BJ. Zn2+ entry produces oxidative neuronal necrosis in cortical cell cultures. *Eur J Neurosci*. 1999;11:327–334.
33. Kim YH, Koh JY. The role of NADPH oxidase and neuronal nitric oxide synthase in zinc-induced poly(ADP-ribose) polymerase activation and cell death in cortical culture. *Exp Neurol*. 2002;177:407–418.
34. Ripps H, Chappell RL. Review: zinc's functional significance in the vertebrate retina. *Mol Vis*. 2014;20:1067–1074.
35. Ugarte M, Osborne NN, Brown LA, Bishop PN. Iron, zinc, and copper in retinal physiology and disease. *Surv Ophthalmol*. 2013;58:585–609.
36. Lowe NM, Fekete K, Decsi T. Methods of assessment of zinc status in humans: a systematic review. *Am J Clin Nutr*. 2009; 89:2040S–2051S.
37. Michaluk P, Kaczmarek L. Matrix metalloproteinase-9 in glutamate-dependent adult brain function and dysfunction. *Cell Death Differ*. 2007;14:1255–1258.
38. De Groef L, Andries L, Lemmens K, Van Hove I, Moons L. Matrix metalloproteinases in the mouse retina: a comparative study of expression patterns and MMP antibodies. *BMC Ophthalmol*. 2015;15:187.
39. Mathalone N, Lahat N, Rahat MA, Bahar-Shany K, Oron Y, Geyer O. The involvement of matrix metalloproteinases 2 and 9 in rat retinal ischemia. *Graefes Arch Clin Exp Ophthalmol*. 2007;245:725–732.
40. Hwang JJ, Park MH, Choi SY, Koh JY. Activation of the Trk signaling pathway by extracellular zinc: role of metalloproteinases. *J Biol Chem*. 2005;280:11995–12001.
41. Chintala SK. The emerging role of proteases in retinal ganglion cell death. *Exp Eye Res*. 2006;82:5–12.
42. Reichenbach A, Wurm A, Pannicke T, Iandiev I, Wiedemann P, Bringmann A. Müller cells as players in retinal degeneration and edema. *Graefes Arch Clin Exp Ophthalmol*. 2007;245: 627–636.
43. Limb GA, Daniels JT, Pleass R, Charteris DG, Luthert PJ, Khaw PT. Differential expression of matrix metalloproteinases 2 and 9 by glial Müller cells: response to soluble and extracellular matrix-bound tumor necrosis factor-alpha. *Am J Pathol*. 2002; 160:1847–1855.
44. Rodrigues M, Xin X, Jee K, et al. VEGF secreted by hypoxic Müller cells induces MMP-2 expression and activity in endothelial cells to promote retinal neovascularization in proliferative diabetic retinopathy. *Diabetes*. 2013;62:3863–3873.
45. De Groef L, Andries L, Lemmens K, Van Hove I, Moons L. Matrix metalloproteinases in the mouse retina: a comparative study of expression patterns and MMP antibodies. *BMC Ophthalmol*. 2015;15:187.

Investigative Ophthalmology & Visual Science